

Distributed Community Detection for Large Scale Networks Using Stochastic Block Model

Shihao Wu¹, Zhe Li¹, and Xuening Zhu¹

¹*School of Data Science, Fudan University, Shanghai, China*

Abstract

With rapid developments of information and technology, large scale network data are ubiquitous. In this work we develop a distributed spectral clustering algorithm for community detection in large scale networks. To handle the problem, we distribute l pilot network nodes on the master server and the others on worker servers. A spectral clustering algorithm is first conducted on the master to select pseudo centers. The indexes of the pseudo centers are then broadcasted to workers to complete distributed community detection task using a SVD type algorithm. The proposed distributed algorithm has three merits. First, the communication cost is low since only the indexes of pseudo centers are communicated. Second, no further iteration algorithm is needed on workers and hence it does not suffer from problems as initialization and non-robustness. Third, both the computational complexity and the storage requirements are much lower compared to using the whole adjacency matrix. A Python package DCD (www.github.com/Ikerlz/dcd) is developed to implement the distributed algorithm for a Spark system. Theoretical properties are provided with respect to the estimation accuracy and mis-clustering rates. Lastly, the advantages of the proposed methodology are illustrated by experiments on a variety of synthetic and empirical datasets.

KEY WORDS: Large scale network; Community detection; Distributed spectral clustering; Stochastic block model; Distributed system.

*Shihao Wu and Zhe Li are joint first authors. Xuening Zhu is corresponding author (xueningzhu@fudan.edu.cn). Xuening Zhu is supported by the National Natural Science Foundation of China (nos. 11901105, 71991472, U1811461), the Shanghai Sailing Program for Youth Science and Technology Excellence (19YF1402700), and the Fudan-Xinzailing Joint Research Centre for Big Data, School of Data Science, Fudan University.

1. INTRODUCTION

Large scale networks have become more and more popular in today's world. Recently, network data analysis receives great attention in a wide range of applications, which include but not limited to social network analysis (Sojourner, 2013; Liu et al., 2017; Zhu et al., 2020), biological study (Marbach et al., 2010, 2012), financial risk management (Härdle et al., 2016; Zou et al., 2017) and many others.

Among the existing literature for large scale network data, the stochastic block model (SBM) is widely used due to its simple form and great usefulness (Holland et al., 1983). In a SBM, the network nodes are partitioned into K communities according to their connections. Within the same community, nodes are more likely to form edges with each other. On the other hand, the nodes from different communities are less likely to form connections. Understanding the community structure is vital in a variety of fields. For instance, in social network analysis, users from the same community are likely to share similar social interests. As a consequence, particular marketing strategies can be applied based on their community memberships.

Statistically, the communities in the SBM are latent hence need to be detected. One of the most fundamental problems in the SBM is to recover community memberships from the observed network relationships. To address this issue, researchers have proposed various estimation methods to accomplish this task. For instance, Zhao et al. (2012), Amini et al. (2013) and Bickel and Chen (2009) adopted likelihood based methods and proved asymptotic properties. Other approaches include convex optimization (Chen et al., 2012), methods of moments (Anandkumar et al., 2014), spectral clustering (Lei and Rinaldo, 2015; Jin et al., 2015; Lei et al., 2020) and many others.

Among the approaches, spectral clustering (Von Luxburg, 2007; Balakrishnan et al.,

2011; Rohe et al., 2011; Lei and Rinaldo, 2015; Jin et al., 2015; Sarkar et al., 2015; Lei et al., 2020) is one of the most widely used methods for community detection. Particularly, it first performs eigen-decomposition using the adjacency matrix or the graph Laplacian matrix. Then the community memberships are estimated by further applying a k -means algorithm to the first several leading eigenvectors. Theoretically, both Rohe et al. (2011) and Lei and Rinaldo (2015) have studied the consistency of spectral clustering under stochastic block models.

Despite the usefulness of spectral clustering on community detection problem, the procedure is computationally demanding especially when the network is of large scale. In the meanwhile, with rapid developments of information and technology, large scale network data are ubiquitous. On one hand, handling such enormous datasets requires great computational power and storage capacity. Hence, it is nearly impossible to complete statistical modelling tasks on a central server. On the other hand, the concerns of privacy and ownership issues require the datasets to be distributed across different data centers. In the meanwhile, due to the distributed storage of the datasets, constraints on communication budgets also post great challenges on statistical modelling tasks. Therefore, developing distributed statistical modelling methods which are efficient with low computation and communication cost is important.

In recent literature, a surge of researches have emerged to solve the distributed statistical modelling problems. For instance, to conduct distributed regression analysis, both one-shot and iterative distributed algorithms are designed and studied (Zhang et al., 2013; Liu and Ihler, 2014; Chang et al., 2017a,b). Furthermore, high-dimensional sparse learning problems are investigated and corresponding asymptotic properties are established (Lee et al., 2015; Battey et al., 2015; Jordan et al., 2018; Zhu et al., 2019). Other than the supervised learning tasks, distributed semi-supervised and unsupervised

learning methods are also studied (Chang et al., 2017a; Fan et al., 2017). However, due to our best knowledge, none of the above literature could tackle distributed community detection problems for large scale networks.

In this work, we propose a distributed community detection (DCD) algorithm. The distributed system typically consists of a master server and multiple worker servers. In each round of computation, the master server is responsible to broadcast tasks to workers, then the workers conduct computational tasks using local datasets and communicate the results to the master. More specifically, we distribute the network nodes together with their network relationships on both masters and workers. Specifically, on the master server we distribute l network nodes, who are referred to as *pilot nodes*. The network relationships among the pilot nodes are stored on the master server. On the m th worker, we distribute n_m network nodes together with l pilot nodes. The network relationships between the n_m network nodes and the pilot nodes are recorded. Compared to storing the whole network relationships, we resort to storing only a partial network, which leads to much lower storage requirements.

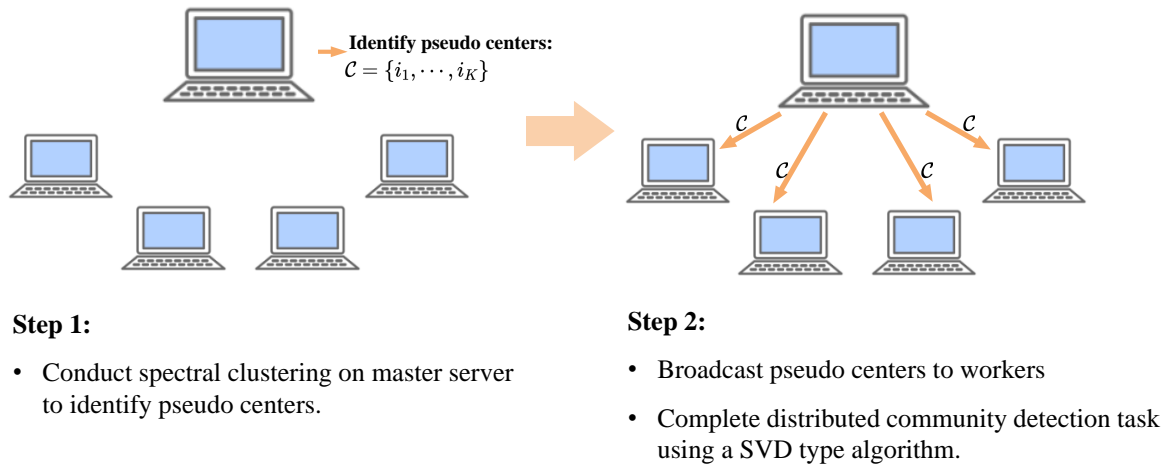


Figure 1: Illustration of distributed community detection algorithm. One time communication is required between master and workers.

The distributed community detection is then conducted as follows. First, we perform a spectral clustering on the master server using l pilot nodes. During this step, K *pseudo centers* are identified. The pseudo centers are identified as the pilot nodes most close to the clustering centers. Next, we broadcast the indexes of the pseudo centers to workers to further complete the community detection task by using a SVD type algorithm. The basic steps of the algorithm are summarized in Figure 1. The algorithm has the following three merits. First, the communication cost is low since only the indexes of pseudo centers are communicated and only one time communication is used. Second, no further iteration algorithm is needed on workers and hence it does not suffer from problems as initialization and non-robustness. Third, the total computational complexity is of order $O(Ml^3 + \sum_{m=1}^M n_m l^2)$, where M is the number of workers. Therefore the computational cost is low as long as the size of pilot nodes is well controlled. We would like to remark that the proposed algorithm can be applied not only on distributed systems, but also on a single computer with memory constraint. Theoretically, we establish upper bounds of (a) the singular vector estimation error and (b) the number of mis-clustering nodes. Extensive numerical study is presented to illustrate the computational power of the proposed methodology.

The article is organized as follows. In Section 2, we introduce stochastic block model and our distributed community detection algorithm. In Section 3, we develop the theoretical properties of the estimation accuracies of the community detection task. In Section 4 and 5, we study the performance of our algorithm via simulation and real data analysis. Section 6 concludes the article with a discussion. All proofs and technique lemmas are relegated to the Appendix.

2. DISTRIBUTED SPECTRAL CLUSTERING FOR STOCHASTIC BLOCK MODEL

2.1. Stochastic Block Model and Spectral Clustering

Consider a large scale network with N nodes, which can be clustered into K communities. For each node i , let $g_i \in \{1, \dots, K\}$ be its community label. A stochastic block model is parameterized by a *membership matrix* $\Theta = (\Theta_1, \dots, \Theta_N)^\top \in \mathbb{R}^{N \times K}$ and a *connectivity matrix* $B \in \mathbb{R}^{K \times K}$ (with full rank). For the i th row of Θ , only the g_i th element takes 1 and the others are 0. In addition, the connectivity matrix B characterizes the connection probability between communities. Specifically, the connection probability between the k th and l th community is B_{kl} . The edge A_{ij} between the node i and j is generated independently from Bernoulli($B_{g_i g_j}$) distribution. The adjacency matrix is then defined as $A = (A_{ij})$. By using the adjacency matrix, the Laplacian matrix L can be defined as $L = D^{-1/2} A D^{-1/2}$, where D is a diagonal matrix with the i th diagonal element being $D_{ii} = \sum_j A_{ij}$.

Define $\mathcal{A} = \mathbb{E}(A)$ and $\mathcal{D} = \mathbb{E}(D)$ as the population leveled counterparts of A and D . Accordingly let $\mathcal{L} = \mathcal{D}^{-1/2} \mathcal{A} \mathcal{D}^{-1/2}$. For a matrix $X \in \mathbb{R}^{m \times n}$, denote $X_i \in \mathbb{R}^n$ as the i th row of matrix X . The following Lemma shows the connection between the membership matrix and the eigenvector matrix of \mathcal{L} .

Lemma 1. *The eigen-decomposition of \mathcal{L} takes the form $\mathcal{L} = U \Lambda U^\top$, where $U = (U_1, \dots, U_N)^\top \in \mathbb{R}^{N \times K}$ collects the eigen-vectors and $\Lambda \in \mathbb{R}^{K \times K}$ is a diagonal matrix. Further we have $U = \Theta \mu$, where μ is a $K \times K$ orthogonal matrix and $\Theta_i = \Theta_j$ if and only if $U_i = U_j$.*

The proof of Lemma 1 is given by [Rohe et al. \(2011\)](#). By Lemma 1, it can be concluded that U only has K distinct rows and the i th row is equal to the j th row if the corresponding two nodes belong to the same community. Accordingly, let $\widehat{U} \in \mathbb{R}^{N \times K}$ denote the K eigenvectors of L with top K absolute eigenvalues. Under mild conditions,

one can show that \hat{U} is a slightly perturbed version of U and thus has roughly K distinct rows as well. Applying a k -means clustering algorithm to \hat{U} , we are then able to estimate the membership matrix. The spectral clustering algorithm is summarized in Algorithm 1.

Algorithm 1 Spectral Clustering for SBM

Input: Adjacency matrix A ; number of communities K ; approximation error ε .

Output: Membership matrix $\hat{\Theta}$.

- 1: Compute Laplacian matrix L based on A .
 - 2: Conduct eigen-decomposition of L and extract the top K eigenvectors (i.e., \hat{U}).
 - 3: Conduct k -means algorithm using \hat{U} and then output the estimated membership matrix $\hat{\Theta}$.
-

Despite the usefulness, the classical spectral clustering method for the SBM is computationally intensive with computational complexity in the order $O(N^3)$. Hence it is hard to apply in the large scale networks. In the following we aim to develop a distributed spectral clustering algorithm for the SBM model. Specifically, we first introduce a pilot network spectral clustering algorithm on the master server in Section 2.2. Then we elaborate the communication mechanism and computation on workers for the distributed community detection task in Section 2.3 and Section 2.4.

2.2. Pilot Network Spectral Clustering on Master Server

For the distributed community detection task, we first conduct a pilot-based spectral clustering on the master server. Suppose we have l network nodes on the master, which are referred to as *pilot nodes*. In addition we distribute the pilot nodes both on

master and workers. In the distributed system, the adjacency matrix is distributed as in Figure 2. As a result, compared to storing the whole network relationships, only a sub-adjacency matrix (i.e., partial network) is stored. This leads to a much lower storage requirement.

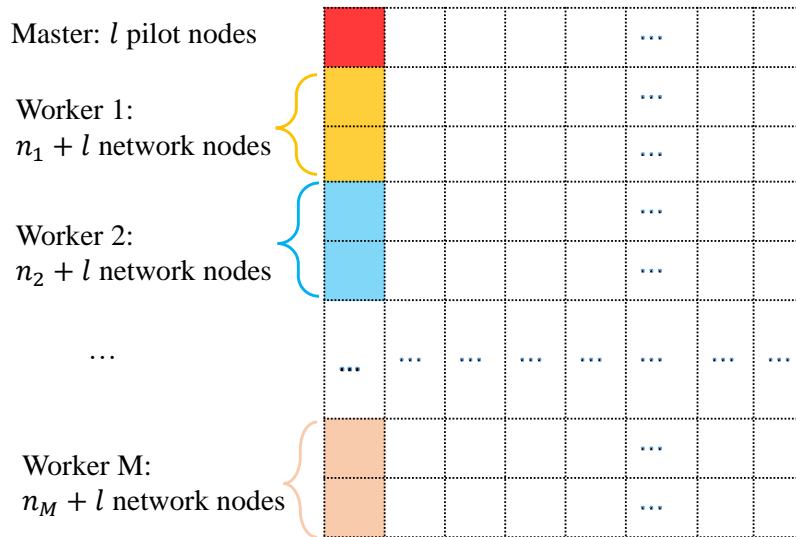


Figure 2: Distributed adjacency matrix A in the distributed system. On master server, l pilot nodes are distributed. On the m th worker, the network relationships between the $n_m + l$ network nodes and pilot nodes are stored.

Let $m_k = \sum_{i=1}^N I(g_i = k)$ be the number of nodes in the k th community. In addition, define n_{0k} be the number of pilot nodes in the k th community. Without loss of generality, we assume $n_{0k}/m_k = r_0$ for $k = 1, \dots, K$. Consequently, the relative size of each community (i.e. distribution of memberships) is the same for the pilot nodes.

Subsequently, define the adjacency matrix among the pilot nodes as $A_0 \in \mathbb{R}^{l \times l}$. Denote the corresponding Laplacian matrix L_0 as $L_0 = D_0^{-1/2} A_0 D_0^{-1/2}$, where $D_0 = \text{diag}\{D_{0,11}, \dots, D_{0,ll}\}$ with $D_{0,ii} = \sum_j A_{0,ij}$. Accordingly, define $\mathcal{D}_0 = E(D_0)$, $\mathcal{A}_0 = E(A_0)$, and $\mathcal{L}_0 = \mathcal{D}_0^{-1/2} \mathcal{A}_0 \mathcal{D}_0^{-1/2}$.

By Lemma 3.1 in [Rohe et al. \(2011\)](#), the eigen-decomposition of \mathcal{L}_0 takes the form as $\mathcal{L}_0 = U_0 \Lambda_0 U_0^\top$, where $\Lambda_0 \in \mathbb{R}^{K \times K}$ and $U_0 \in \mathbb{R}^{l \times K}$ has K distinct rows. We collect the K distinct rows in the matrix $U_0^{(K)} \in \mathbb{R}^{K \times K}$. In addition, let $U^{(K)}$ collect K distinct rows of U . The following proposition establishes the relationship between $U_0^{(K)}$ and $U^{(K)}$.

Proposition 1. *Under the assumption that $n_{0k}/m_k = r_0$ for $k = 1, \dots, K$, we have $U_0^{(K)} = r_0^{-1/2} U^{(K)}$.*

The proof of Proposition 1 is given in Appendix B.1. By Proposition 1, it could be concluded that $U_0^{(K)}$ is equivalent to $U^{(K)}$ up to a ratio $r_0^{-1/2}$. Empirically, by conducting a spectral clustering algorithm on the master, we are able to cluster the pilot nodes correctly with a high probability ([Rohe et al., 2011](#)).

2.3. Pseudo Centers and Communication Mechanism

After clustering pilot nodes on the master, we then broadcast the clustering results to workers to further complete community detection on workers. To conduct the task, K *pseudo centers* are selected for broadcasting as in Step 2 of Algorithm 2. To be more specific, define the clustering centers of \widehat{U}_0 (eigenvector matrix of L_0) after the k -means algorithm as $\widehat{C}_0 = (\widehat{C}_{0k} : 1 \leq k \leq K)^\top$. Then the index of the k th pseudo center is defined by $i_k = \arg \min_i \|\widehat{U}_{0i} - \widehat{C}_{0k}\|$, which is the closest node to the center of the k th cluster. The pseudo centers are *pseudo* in the sense that they are not exactly the clustering centers but the closest nodes to the centers. As a result, they could be treated as the most representative nodes for each community. The indexes of pseudo centers are recorded as $\mathcal{C} = \{i_1, \dots, i_K\}$.

Remark 1. Note that in the communication step, we only broadcast the indexes of pseudo centers instead of clustering centers \widehat{C}_0 . There are two advantages for doing

so. First, the communication cost is low compared to broadcasting \widehat{C}_0 . Specifically, only K integers need to be communicated. Second, even though the clustering center matrix \widehat{C}_0 is broadcasted, we still need to know a rotation matrix for further clustering on workers. Instead, by broadcasting pseudo centers, we no longer need to estimate the rotations but only use the pseudo center indexes on workers. The detailed procedure is presented in the next section.

2.4. Community Detection on Workers

Suppose we distribute n_m network nodes as well as the pilot nodes on the m th worker. Let \mathcal{P} collect the indexes of pilot nodes and \mathcal{M}_m collect the indexes of n_m network nodes on the m th worker. Denote $\mathcal{S}_m = \mathcal{P} \cup \mathcal{M}_m$ with $|\mathcal{S}_m| = \bar{n}_m$, where $\bar{n}_m = l + n_m$. Particularly on the m th worker, we store the network relationships between nodes in \mathcal{S}_m and the pilot nodes in \mathcal{P} . Denote the corresponding sub-adjacency matrix as $A^{(\mathcal{S}_m)} \in \mathbb{R}^{\bar{n}_m \times l}$. Without loss of generality, we permute the row indexes of $A^{(\mathcal{S}_m)}$ to ensure that $A^{(\mathcal{S}_m)} = (A_1^{(\mathcal{S}_m)\top}, A_2^{(\mathcal{S}_m)\top})^\top$ with $A_1^{(\mathcal{S}_m)} = A_0$. As a result, the first l rows of $A^{(\mathcal{S}_m)}$ (i.e., $A_1^{(\mathcal{S}_m)}$) store the adjacency matrix for the pilot nodes, and the rest (i.e., $A_2^{(\mathcal{S}_m)}$) records the network relationship between the other n_m nodes (i.e., \mathcal{M}_m) and the l pilot nodes.

Let $D_{ii}^{(\mathcal{S}_m)} = \sum_j A_{ij}^{(\mathcal{S}_m)}$ and $F_{jj}^{(\mathcal{S}_m)} = \sum_i A_{ij}^{(\mathcal{S}_m)}$ be the out- and in-degrees of node i and j in the subnetwork on worker m . Correspondingly, define $D^{(\mathcal{S}_m)} = \text{diag}\{D_{ii}^{(\mathcal{S}_m)} : 1 \leq i \leq \bar{n}_m\} \in \mathbb{R}^{\bar{n}_m \times \bar{n}_m}$ and $F^{(\mathcal{S}_m)} = \text{diag}\{F_{jj}^{(\mathcal{S}_m)} : 1 \leq j \leq l\} \in \mathbb{R}^{l \times l}$. Then a Laplacian version of $A^{(\mathcal{S}_m)}$ is given by $L^{(\mathcal{S}_m)} = (D^{(\mathcal{S}_m)})^{-1/2} A^{(\mathcal{S}_m)} (F^{(\mathcal{S}_m)})^{-1/2} \in \mathbb{R}^{\bar{n}_m \times l}$.

Given the Laplacian matrix, we further perform the clustering algorithm on workers. First, we conduct a singular value decomposition (SVD) using $L^{(\mathcal{S}_m)}$. Note that the SVD can be done very efficiently as follows. First, we conduct an eigenvalue decom-

position on $L^{(\mathcal{S}_m)\top} L^{(\mathcal{S}_m)} \in \mathbb{R}^{l \times l}$ with computational complexity in the order of $O(l^3)$. This leads to $L^{(\mathcal{S}_m)\top} L^{(\mathcal{S}_m)} = \tilde{V}_m \tilde{\Lambda}_m \tilde{V}_m^\top$, where $\tilde{V}_m \in \mathbb{R}^{l \times l}$ is the right singular vectors of $L^{(\mathcal{S}_m)} \in \mathbb{R}^{l \times l}$ and $\tilde{\Lambda}_m \in \mathbb{R}^{l \times l}$ is a diagonal matrix. Then the left singular vectors can be efficiently computed by $\tilde{U}_m = L^{(\mathcal{S}_m)} \tilde{V}_m \tilde{\Lambda}_m^{-1/2}$ with computational complexity $O(n_m l^2)$. Next, let $\hat{U}^{(\mathcal{S}_m)} \in \mathbb{R}^{\bar{n}_m \times K}$ collect the top K left singular vectors in \tilde{U}_m . Then we assign each node to the cluster with the closest pseudo center. Specifically, recall the indexes of the pseudo centers are collected by $\mathcal{C} = \{i_1, \dots, i_K\}$. As a result, for the i th ($l+1 \leq i \leq \bar{n}_m$) node in \mathcal{S}_m , the cluster label g_i is estimated by

$$\hat{g}_i = \arg \min_{1 \leq k \leq K, i_k \in \mathcal{C}} \|\hat{U}_i^{(\mathcal{S}_m)} - \hat{U}_{i_k}^{(\mathcal{S}_m)}\|^2. \quad (2.1)$$

An obvious merit of (2.1) is that no further iteration algorithms (e.g., k -means) are needed for clustering. It makes the clustering results more stable and computationally efficient. The procedure for community detection on workers is summarized in Step 3 of Algorithm 2.

3. THEORETICAL PROPERTIES

In this section, we discuss the accuracy of the clustering algorithm. We first establish the theoretical properties of the procedure on the population level. Next, the convergence of singular vectors is given, which is the key for establishing the consistent clustering result. Lastly, we derive error bounds on the mis-clustering rates.

Algorithm 2 Distributed Community Detection (DCD) for SBM

Input: Adjacency matrix A_0 ; sub-adjacency matrices $\{A^{(\mathcal{S}_m)}\}_{m=1,\dots,M}$;

number of communities K ; approximation error ε .

Output: Membership matrix $\hat{\Theta}$

STEP 1 PILOT-BASED NETWORK SPECTRAL CLUSTERING ON MASTER
SERVER

STEP 1.1 Conduct eigen-decomposition of L_0 and extract the top K
eigenvectors (denoted in matrix \hat{U}_0).

STEP 1.2 Conduct k -means algorithm and obtain clustering centers
 $\hat{C}_0 = (\hat{C}_{0k} : 1 \leq k \leq K)^\top$.

STEP 2 BROADCAST PSEUDO CENTERS TO WORKERS

STEP 2.1 Determine the indexes of the k th pseudo centers as $i_k =$
 $\arg \min_i \|\hat{U}_{0i} - \hat{C}_{0k}\|_2^2$.

STEP 2.2 Broadcast the index set of pseudo centers $\mathcal{C} = \{i_1, \dots, i_K\}$ to
workers.

STEP 3 COMMUNITY DETECTION ON WORKERS

STEP 3.1 Perform singular value decomposition using $L^{(\mathcal{S}_m)}$ and denote
the top K left singular vector matrix as $\hat{U}^{(\mathcal{S}_m)}$.

STEP 3.2 Use (2.1) to obtain the estimated community labels.

3.1. Theoretical Properties on Population Level

To motivate the study, we first discuss the theoretical properties on the population level. Define $\mathcal{A}^{(\mathcal{S}_m)} = E(A^{(\mathcal{S}_m)})$, $\mathcal{D}^{(\mathcal{S}_m)} = E(D^{(\mathcal{S}_m)}) \in \mathbb{R}^{\bar{n}_m \times \bar{n}_m}$ and $\mathcal{F}^{(\mathcal{S}_m)} = E(F^{(\mathcal{S}_m)}) \in \mathbb{R}^{l \times l}$. In addition, the normalized population adjacency matrix is defined by $\mathcal{L}^{(\mathcal{S}_m)} =$

$(\mathcal{D}(\mathcal{S}_m))^{-1/2} \mathcal{A}(\mathcal{S}_m) (\mathcal{F}(\mathcal{S}_m))^{-1/2}$. Suppose the singular value decomposition of $\mathcal{L}^{(\mathcal{S}_m)}$ is $\mathcal{L}^{(\mathcal{S}_m)} = U^{(\mathcal{S}_m)} \Lambda^{(\mathcal{S}_m)} (V^{(\mathcal{S}_m)})^\top$, where $U^{(\mathcal{S}_m)} \in \mathbb{R}^{\bar{n}_m \times K}$ and $V^{(\mathcal{S}_m)} \in \mathbb{R}^{l \times K}$ are left and right eigenvectors respectively. In the following proposition we show that $U^{(\mathcal{S}_m)}$ has K distinct rows and could identify the memberships of the nodes uniquely.

Proposition 2. *Let $\Theta^{(\mathcal{S}_m)} \in \mathbb{R}^{\bar{n}_m \times K}$ be the membership matrix on the m th worker. Then we have $U^{(\mathcal{S}_m)} = \Theta^{(\mathcal{S}_m)} \mu$, where $\mu \in \mathbb{R}^{K \times K}$ is a rotation matrix, and*

$$\mu^\top \Theta_i^{(\mathcal{S}_m)} = \mu^\top \Theta_j^{(\mathcal{S}_m)} \Leftrightarrow \Theta_i^{(\mathcal{S}_m)} = \Theta_j^{(\mathcal{S}_m)}.$$

Proof of Proposition 2 is given in Appendix B.2. Proposition 2 implies that the singular vectors could play the same role as the eigenvectors of the adjacency matrix in the community detection.

We then build the connection between $U^{(\mathcal{S}_m)}$ with the eigenvector matrix U of \mathcal{L} , i.e., $\mathcal{L} = U \Lambda U^\top$. Denote $U_m = (U_i : i \in \mathcal{S}_m)^\top \in \mathbb{R}^{\bar{n}_m \times K}$ as the submatrix of U whose row indexes are in \mathcal{S}_m . The connection could be built between $U^{(\mathcal{S}_m)}$ and U_m . Denote \bar{n}_{mk} as the number of nodes on the m th worker belonging to the k th community. If we have \bar{n}_{mk}/m_k s are equivalent over $1 \leq k \leq K$. Then it could be easily verified as Proposition 1 that $U^{(\mathcal{S}_m)} = r_m^{-1/2} U_m$, where $r_m = \bar{n}_m / (N + l)$. However, in practice, the distributed nodes on the workers are mostly unbalanced with respect to the whole population. For instance, smaller samples of the k th community may be distributed on the m th worker compared to other workers. As a result, $U^{(\mathcal{S}_m)}$ will not be just equal to $r_m^{-1/2} U_m$.

This unbalanced effect can be quantified in the theoretical analysis. Define the *unbalanced effect* as $\alpha^{(\mathcal{S}_m)} = \max_k |\bar{n}_{mk}/\bar{n}_m - m_k/N|$. As a result, $\alpha^{(\mathcal{S}_m)}$ will be large if the ratio of one community (e.g., the k th community) on the m th worker is far away

from its population ratio m_k/N . In addition, let $d_0 \leq \min_k n_{0k}/l \leq \max_k n_{0k}/l \leq u_0$ and $d_m \leq \min_k n_{mk}/\bar{n}_m \leq \max_k n_{mk}/\bar{n}_m \leq u_m$. We establish an upper bound for the deviation of $U^{(\mathcal{S}_m)}$ from $r_m^{-1/2}U_m$.

Proposition 3. *Let $b_{\min} = \min_{1 \leq i, j \leq K} B_{ij}$. It holds*

$$\|U^{(\mathcal{S}_m)} - r_m^{-1/2}U_m Q_m\|_F \leq \frac{14\sqrt{2}K^2 u_m \max\{u_0^{1/2}, u_m^{1/2}\} \alpha^{(\mathcal{S}_m)1/2}}{\sigma_{\min}(B) b_{\min}^3 d_0^2 d_m^3 (d_0 + d_m)} + \frac{\alpha^{(\mathcal{S}_m)}}{d_0} \quad (3.1)$$

where Q_m is an $K \times K$ orthogonal matrix.

Proof of Proposition 3 is given in Appendix B.3. The upper bound in (3.1) illustrates the relationship between the error bounds and the unbalanced effect. Particularly, the error bound is tighter when the community members are distributed more evenly on each worker. In the extreme case, when the unbalanced effect is 0 (i.e., $\alpha^{(\mathcal{S}_m)} = 0$), the upper bound in (3.1) will be zero.

3.2. Convergence of Singular Vectors

As we have shown previously, $U^{(\mathcal{S}_m)}$ has K distinct rows. As a result, if $\widehat{U}^{(\mathcal{S}_m)}$ converges to $U^{(\mathcal{S}_m)}$ with a high probability, we are able to achieve a high clustering accuracy based on spectral clustering using $\widehat{U}^{(\mathcal{S}_m)}$. In the following theorem we establish the convergence result of $\widehat{U}^{(\mathcal{S}_m)}$ to $U^{(\mathcal{S}_m)}$.

Theorem 1. (SINGULAR VECTOR CONVERGENCE) *Let $\lambda_{1,m} \geq \lambda_{2,m} \geq \dots \geq \lambda_{K,m} > 0$ be the top K singular values of $\mathcal{L}^{(\mathcal{S}_m)}$. Define $\delta_m = \min_i \mathcal{D}_{ii}^{(\mathcal{S}_m)}$. Then for any $\epsilon_m > 0$ and $\delta_m > 3 \log(n_m + 2l) + 3 \log(4/\epsilon_m)$, with probability at least $1 - \epsilon_m$ it holds*

$$\|\widehat{U}^{(\mathcal{S}_m)} - U^{(\mathcal{S}_m)} Q^{(\mathcal{S}_m)}\|_F \leq \frac{8\sqrt{6}}{\lambda_{K,m}} \sqrt{\frac{K \log(4(n_m + 2l)/\epsilon_m)}{\delta_m}}, \quad (3.2)$$

where $Q^{(\mathcal{S}_m)} \in \mathbb{R}^{K \times K}$ is a $K \times K$ orthogonal matrix.

The proof of Theorem 1 is given in Appendix C.1. To better understand the estimation error bound given in (3.2), we make the following comments. First, the error bound is related to $\lambda_{K,m}$. According to Rohe et al. (2011) and Lei and Rinaldo (2015), if $\lambda_{K,m}$ is larger, the eigengap between the eigenvalues of interest and the rest will be higher. This enables us to detect communities with higher accuracy level.

Second, the upper bound is lower if the minimum out-degree δ_m is higher. One could verify that $\mathcal{D}_{ii}^{(\mathcal{S}_m)} = (\Theta_i^{(\mathcal{S}_m)})^\top B \Theta_0^\top \mathbf{1}_l \geq b_{\min} \sum_k n_{0k} = b_{\min} l$. Consequently δ_m grows almost linearly with l if b_{\min} is lower bounded. If $\delta_m \gg K \log \bar{n}_m$ and $\lambda_{K,m}$ is lower bounded by a positive constant, then we have $\|\widehat{U}^{(\mathcal{S}_m)} - U^{(\mathcal{S}_m)} Q^{(\mathcal{S}_m)}\|_F = o_p(1)$. Lastly, the error bound is higher when the number of communities K and the sub-sample size \bar{n}_m is larger. As a result, larger K and \bar{n}_m will increase the difficulty of the community detection task.

3.3. Clustering Accuracy Analysis

In this section, we conduct clustering accuracy analysis for the DCD algorithm. To this end, we first present a sufficient condition, which guarantees correct clustering for a single node. Let $\widehat{C}^{(\mathcal{S}_m)} = (\widehat{C}_1^{(\mathcal{S}_m)}, \dots, \widehat{C}_K^{(\mathcal{S}_m)})^\top \in \mathbb{R}^{K \times K}$ be the pseudo centers on the worker m . Denote $P_m = (2/D_m)^{1/2} - 2\zeta_m$ with $D_m = \max_{1 \leq k \leq K} \bar{n}_{mk}$ and $\zeta_m = \max_{k \in \{1, \dots, K\}} \|Q^{(\mathcal{S}_m)\top} U_{i_k}^{(\mathcal{S}_m)} - \widehat{C}_k^{(\mathcal{S}_m)}\|_2$. Here ζ_m characterizes the distance of the pseudo centers to their population values on worker m . We then have the following proposition.

Proposition 4. *The node i will be correctly clustered (i.e., $\widehat{g}_i = g_i$) as long as*

$$\|\widehat{U}_i^{(\mathcal{S}_m)} - \widehat{C}_{g_i}^{(\mathcal{S}_m)}\|_2 < \frac{P_m}{2}. \quad (3.3)$$

The proof of Proposition 4 is given in Appendix B.4. It indicates that the clustering accuracy is closely related to P_m . If with a high probability that the pseudo nodes are correctly clustered, then P_m will be higher. As a consequence, it could yield a higher accuracy of the community detection result.

In the following we analyze the lower bound of P_m . If we could prove that P_m is positive with a high probability, we are then able to show that the total number of mis-clustered nodes are well controlled. Specifically, define the pseudo centers on the master node as $\widehat{U}_{0c} \stackrel{\text{def}}{=} (\widehat{U}_{0i} : i \in \mathcal{C})^\top \in \mathbb{R}^{K \times K}$. Ideally, we could directly map \widehat{U}_{0c} to the column space of $\widehat{U}^{(\mathcal{S}_m)}$ and then complete the community detection on workers. To this end, a rotation Q_c should be made on the pseudo centers of the master node (i.e., \widehat{U}_{0c}). According to Proposition 3 and Theorem 1, rotation Q_c takes the form $Q_c = r_m^{-1/2} r_0^{1/2} Q_0^\top Q_m Q^{(\mathcal{S}_m)}$. As a result, the pseudo centers on the m th worker is defined as $\widehat{C}^{(\mathcal{S}_m)} = \widehat{U}_{0c} Q_c$. To establish a lower bound for P_m , we first assume the following conditions.

- (C1) (EIGENVALUE AND EIGENGAP ON MASTER) Let $\delta_0 = \min_i \mathcal{D}_{0,ii}$. Assume $\delta_0 > 3 \log(2l) + 3 \log(4/\epsilon_l)$ and $\epsilon_l \rightarrow 0$ as $l \rightarrow \infty$.
- (C2) (PILOT NODES) Assume $K^2 \log(l/\epsilon_l)/(b_{\min} \lambda_{K,0}^2) \ll l$ with $\epsilon_l \rightarrow 0$ as $l \rightarrow \infty$.
- (C3) (UNBALANCED EFFECT) Let d_0, d_m, u_0, u_m be finite constants and assume $\alpha^{(\mathcal{S}_m)} = o(\sigma_{\min}(B)^2/K^4)$.

Condition (C1) is imposed by assuming the same condition as in Theorem 1 for the pilot nodes. Condition (C2) gives a lower bound on the number of pilot nodes. Specifically, it should be larger than both the number of communities K and $(\log l)^2/b_{\min}^4$, which is easy to satisfy in practice.

Condition (C3) restricts the unbalanced effect. First, it states that the relative ratio of communities across all workers are stable by assuming d_0, d_m, u_0, u_m are constants. Next, the unbalanced effect $\alpha^{(S_m)}$ is assumed to converge to zero faster than $O(1/K^2)$. As a result, as long as K is well controlled (for instance, in the order of $\log N$) and signal strength in B is strong enough, the conditions (C2) and (C3) could be easily satisfied. We then have the following Proposition.

Proposition 5. *Assume Conditions (C1)–(C3). Then with probability $1 - \epsilon_l$, we have $P_m \geq c_1/\sqrt{n_m}$ as $\min\{l, n_m\} \rightarrow \infty$ with rotation Q_c , where c_1 is a positive constant.*

The proof of Proposition 5 is given in Appendix B.5. In practice, to save us the effort of estimating the rotation matrix Q_c , we directly broadcast the pseudo center indexes \mathcal{C} to workers and let $\widehat{C}^{(S_m)} = (\widehat{U}_i^{(S_m)} : i \in \mathcal{C})^\top$. As a result, $\widehat{C}^{(S_m)}$ is naturally embedded in the column space of $\widehat{U}^{(S_m)}$ and no further rotation is required. Given the results presented in Theorem 1 and Proposition 5, we are then able to obtain the mis-clustering rates for each worker as follows.

Theorem 2. (BOUND OF MIS-CLUSTERING RATES) *Assume conditions in Theorem 1 and Proposition 5. Denote $\mathcal{R}^{(S_m)}$ as the ratio of misclustered nodes on worker m , then we have*

$$\mathcal{R}^{(S_m)} = o\left(\frac{K^2 \log(l/\epsilon_l)}{b_{\min} l \lambda_{K,0}^2} + \frac{K \log(4(n_m + 2l)/\epsilon_m)}{\lambda_{K,m} \delta_m} + \frac{K^4 \alpha^{(S_m)}}{\sigma_{\min}(B)^2 b_{\min}^6}\right), \quad (3.4)$$

with probability at least $1 - \epsilon_l - \epsilon_m$.

The proof of Theorem 2 is given in Appendix C.2. Theorem 2 establishes an upper bound for the mis-clustering rate on the worker m . With respect to the result, we have the following remark.

Remark 2. One could observe that there are three terms included in the mis-clustering rate. The first and second terms are related to convergence of spectrum on master and workers. Specifically, the first term is related to the convergence of eigenvectors on the master. The second term is determined by convergence of singular vectors on the m th worker. As we comment before, with large sample size and strong signal strength, the mis-clustering rate could be well controlled. Next, the third term is mainly related to the unbalanced effect $\alpha^{(\mathcal{S}_m)}$ among the workers, which is lower if the distribution of the communities is more balanced on different workers.

Compared with using the full adjacency matrix of \mathcal{S}_m , the error bound in (3.4) is higher. That is straightforward to understand since in our case we use a sub-adjacency matrix instead of the full one. According to [Rohe et al. \(2012\)](#), when the full adjacency matrix is used, the mis-clustering rate is bounded by $\mathcal{R}_{all}^{(\mathcal{S}_m)} = O(K \log(\bar{n}_m/\epsilon_m)/(\bar{n}_m \lambda_{K,m}^2))$ with high probability. In our case, we have $\mathcal{R}^{(\mathcal{S}_m)} = O(\mathcal{R}_{all}^{(\mathcal{S}_m)} \bar{n}_m/l)$. Hence if it holds $n_m \ll l$ (i.e., $\bar{n}_m \approx l$), then the mis-clustering rate is asymptotically the same as using the full adjacency matrix. Furthermore, we can obtain a mis-clustering error bound for all network nodes as in the following corollary.

Corollary 1. *Assume the same conditions as in Theorem 2. In addition, assume $n_1 = n_2 = \dots = n_M \stackrel{\text{def}}{=} n$ and $\alpha^{(\mathcal{S}_m)} = 0$ for $1 \leq m \leq M$. Denote \mathcal{R}_{all} as number of all mis-clustered nodes across all workers. Then with probability $1 - (M + 1)/l$ we have*

$$\mathcal{R}_{all} = O\left(\frac{K(\log n + \log l)}{l \lambda_K^2}\right), \quad (3.5)$$

where $\lambda_K = \min_m \lambda_{K,m}$.

The Corollary 1 could be immediately obtained from Theorem 2 by setting $\epsilon_l = \epsilon_m = 1/l$ for $1 \leq m \leq M$. As indicated by (3.5), the mis-clustering rate is smaller

when the number of pilot nodes l is larger. Particularly, if $l = rN$ with $r \in (0, 1)$ being a finite positive constant, then the mis-clustering rate is almost the same as we use the whole adjacency matrix A . While in the same time, the computational time is roughly r^2 smaller than using the whole adjacency matrix. As a consequence, the computational advantage is obvious.

4. SIMULATION STUDIES

4.1. Simulation Models and Performance Measurements

In order to demonstrate the performance of our DCD algorithm, we conduct experiments using synthetic datasets under three scenarios. The main differences lie in the generating mechanism of the networks. For simplicity, we consider a stochastic block model with K blocks and each block contains s nodes. As a result, $Ks = N$. The connectivity matrix B is set as

$$B = \nu\{\lambda I_K + (1 - \lambda)\mathbf{1}_K\mathbf{1}_K^\top\}, \quad (4.1)$$

where $\nu \in [0, 1]$ and $\lambda \in [0, 1]$. By (4.1), the connection intensity is then parameterized by ν and the connection divergence is characterized by λ .

The random experiments are repeated for $R = 500$ times for a reliable evaluation. To gauge the finite sample performance, we consider two accuracy measures. The first is the mis-clustering rate, i.e., $\mathcal{R}_{all} = \sum_{i=1}^N (\hat{g}_i \neq g_i) / N$. The second is the estimation accuracy of the singular vectors, i.e., $\hat{U}^{(S_m)}$ for each worker, which is captured by the log-estimation error (LEE). Define $\text{LEE}_m = \log \|\hat{U}^{(S_m)} - U^{(S_m)} Q^{(S_m)}\|_F$ for the m th worker, where the rotation matrix $Q^{(S_m)}$ is calculated according to [Rohe et al. \(2011\)](#).

Subsequently $LEE = M^{-1} \sum_m LEE_m$ is calculated to quantify the average estimation errors over all workers.

4.2. Simulation Results

SCENARIO 1 (PILOT NODES) First, we investigate the role of pilot nodes on the numerical performances. Particularly, we let $l = rN$ with $N = 10000$ and r varying from 0.01 to 0.2. The performances are evaluated for $K = 3, 4, 5, 6$ and the connection intensity and divergence are fixed as $\nu = 0.2$, $\lambda = 0.5$. In addition, the number of workers is given as $M = 5$. We calculated the mis-clustering rate \mathcal{R}_{all} in the left panel of Figure 3. As shown in Figure 3, the mis-clustering rate converges to zero as l grows, which corroborates with our theoretical findings in Corollary 1.

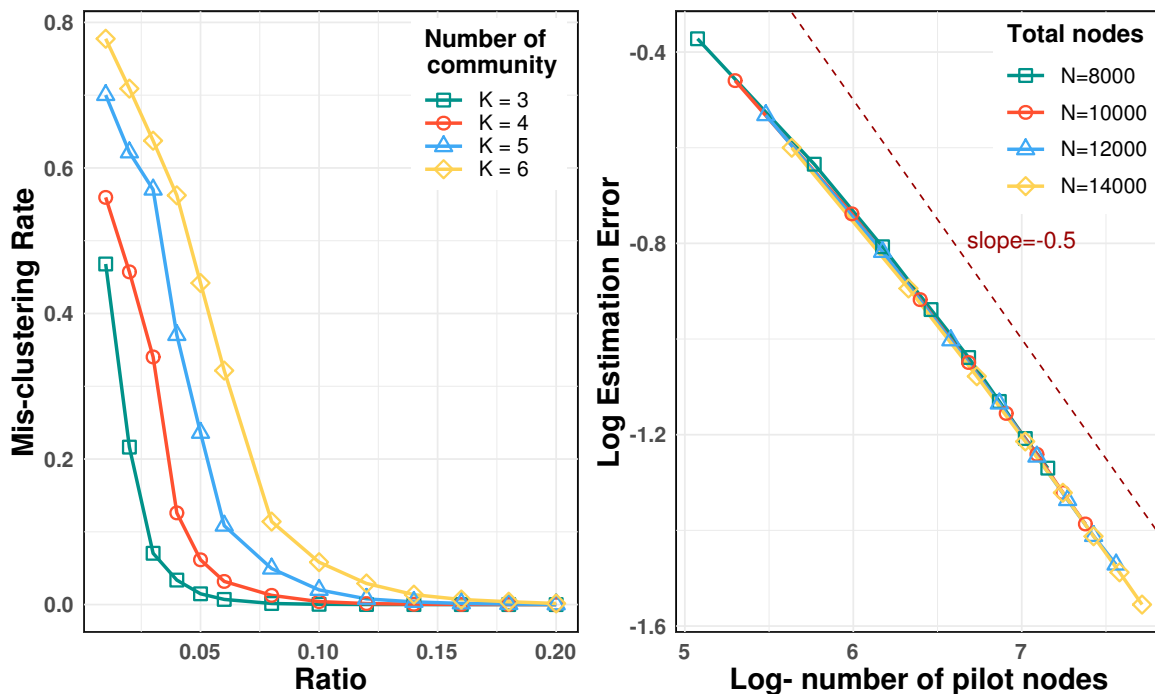


Figure 3: Left panel: the mis-clustering rates versus pilot nodes ratio (i.e., l/N) under different community sizes $K = 3, 4, 5, 6$; Right panel: LEE versus the log-number of pilot nodes under sample sizes $N = 8000, 10000, 12000, 14000$.

Moreover, we evaluate the estimation accuracy of the estimated eigenvectors by

LEE. As we can see from the right panel of Figure 3, for a fixed N , as $\log(l)$ grows, the estimation error of eigenvectors decreases with the slope of LEE roughly parallel with $-1/2$. This corroborates with the theoretical results in Theorem 1.

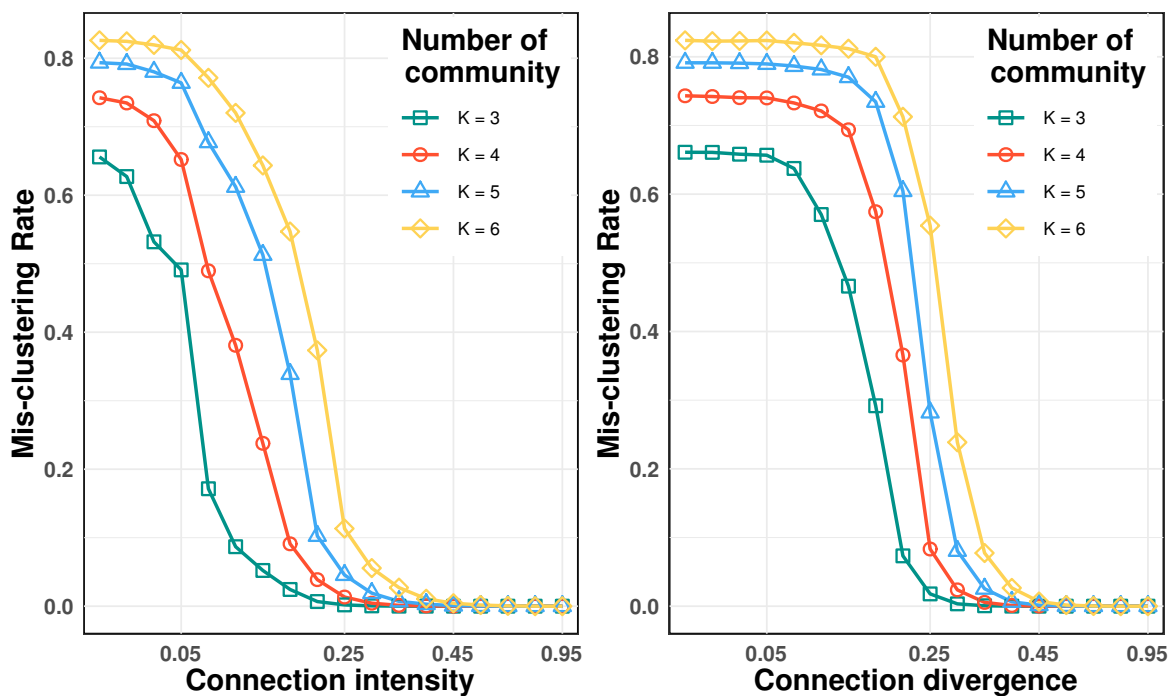


Figure 4: The influence of ν (connection intensity) and λ (connection divergence) on the mis-clustering rates. As shown in the figure, stronger connection and larger divergence can lead to more accurate community detection results.

SCENARIO 2 (SIGNAL STRENGTH) In this scenario, we observe how the mis-clustering rates change with respect to the signal strengths. Accordingly we fix $l = 300$, $N = 20000$, and vary the number of communities as $K = 3, 4, 5, 6$. For $\nu = 0.2$, we first change the connection divergence from $\lambda = 0.05$ to $\lambda = 0.95$. As λ increases, the connection intensity within the same community will be higher than nodes from different communities. In the meanwhile, the eigengap is larger and the signal strength is higher. Next, we conduct the experiment by varying connection intensity ν and fix $\lambda = 0.5$. Theoretically, as ν increases, b_{\min} will increase accordingly, which results in a higher signal strength. According to Theorem 1 and Corollary 1, the mis-clustering

rates will drop as the signal strength is higher. This phenomenon can be confirmed from the right panel of Figure 4.

SCENARIO 3 (UNBALANCED EFFECT) In this setting, we verify the unbalanced effect on the finite sample performances. First, we fix $l = 500$, $N = 5000$, $\nu = 0.2$, $\lambda = 0.5$, and $M = 3$. Denote π_{mk} as the ratio of nodes in the k th community on the m th worker. We set π_{mk} as follows,

$$\pi_{mk} = \frac{1}{K} + \left(k - \frac{K+1}{2}\right) \text{sign}\left(m - \frac{M+1}{2}\right) \frac{\alpha}{K(K-1)}.$$

If $\pi_{m1} = \pi_{m2} = \dots = \pi_{mK} = 1/K$, then there is no unbalanced effect. As α increases, the unbalanced effect is larger. The mis-clustering rate is visualized in Figure 5. As α is increased from 0 to 0.95, we could observe that the mis-clustering rates increase accordingly, which verifies the result of Theorem 2.

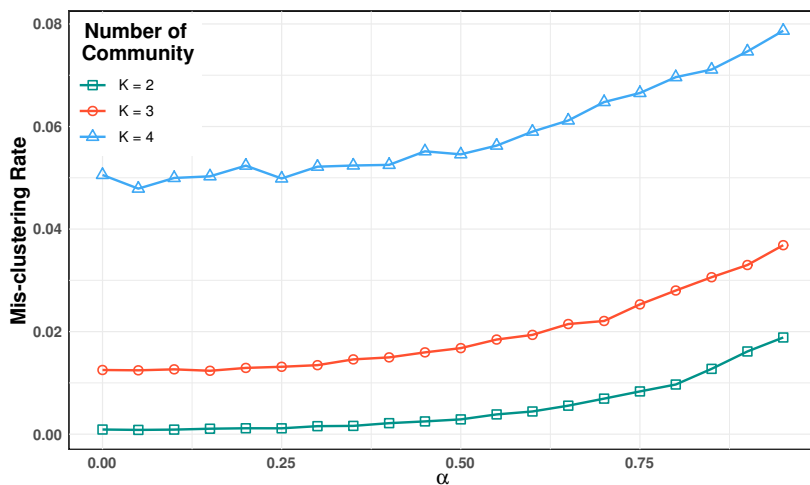


Figure 5: The mis-clustering rates versus the unbalanced effect α for different number of communities $K = 2, 3, 4$. As the unbalanced effect increases, the mis-clustering rates also increase, which results in inferior performance of the distributed algorithm.

4.3. Comparison to Spectral Clustering Algorithm

Lastly, we compare the performances of the proposed method with the spectral

clustering (SC) using the whole network data. Both the mis-clustering rates and the computational efficiency are compared. For a network with size N , we conduct spectral clustering in Algorithm 1 and record the clustering accuracy and computational time. For comparison, we conduct distributed spectral clustering using M workers by Algorithm 2.

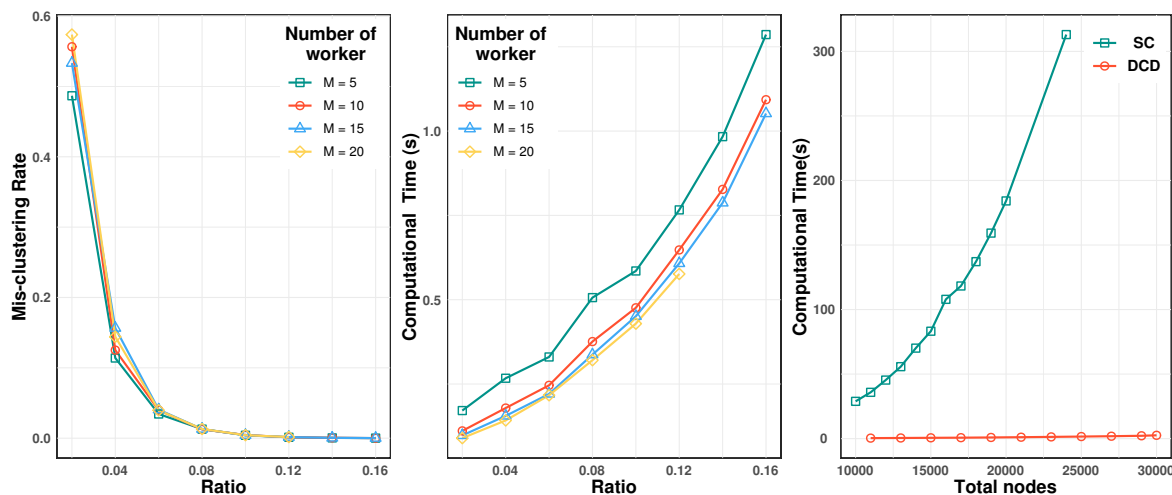


Figure 6: The mis-clustering rates (left panel) and computational time (middle panel) with respect to varying pilot nodes ratios for different number of workers. The computational times of SC Algorithm 1 and DCD Algorithm 2 are further compared as N grows (right panel).

For $N = 10000$ and $K = 3$, the average computational time of spectral clustering Algorithm 1 (using whole network adjacency matrix) is 48.84s and the mis-clustering rate is zero. Next, we set $l = rN$ with $r = 0.02, 0.04, \dots, 0.18$ for Algorithm 2. Both mis-clustering rates and computational time are compared, which is shown in Figure 6. As we could observe, after $l \geq 0.10 \times 10000 = 1000$, our algorithm could obtain the same mis-clustering rate but with much lower computational cost (less than 1 second). In addition, with more workers, the computational cost will be further reduced. Lastly, we compare the computational times as N grows. For each N , l is set when the mis-clustering rate is the same as using the whole adjacency matrix. As we can observe from the right panel of Figure 6, as the network size grows, the computational time

of Algorithm 1 increases drastically compared to Algorithm 2, which illustrates the computational advantage of the proposed approach.

5. EMPIRICAL STUDY

We evaluate the empirical performance of the proposed method using two network datasets. The estimation accuracy and computational time are evaluated using both distributed community detection algorithm and spectral clustering method. Particularly, the distributed community detection algorithm is implemented using our newly developed package DCD on the Spark system. The system consists 36 virtual cores and 128 GB of RAM. We set the number of workers as $M=2$. Descriptions of the two network datasets and corresponding experimental results are presented as follows.

5.1. Pubmed Dataset: a Citation Network

The Pubmed dataset consists of 19,717 scientific publications from PubMed database (Kipf and Welling, 2016). Each publication is identified as one of the three classes, i.e., Diabetes Mellitus Experimental, Diabetes Mellitus Type 1, Diabetes Mellitus Type 2. The sizes of the three classes are 4,103, 7,875, and 7,739 respectively. In this case the community sizes are relatively unbalanced since both the second and third classes have roughly twice members than the first class. The network link is defined using the citation relationships among the publications. Specifically, if the i th publication cites the j th one (or otherwise), then $A_{ij} = 1$, otherwise $A_{ij} = 0$. The resulting network density is 0.028%.

For the Pubmed datasets, we could calculate the mis-clustering rates by using pre-specified class labels as ground truth. The mis-clustering rates of using SC with the whole network are 33.03%. For comparison, the DCD algorithm is evaluated by varying

$r = l/N$ from 0.02 to 0.30. One could observe in Figure 7 that, the mis-clustering rates of the DCD algorithm is comparable to the SC algorithm when $r = 0.22$, while the computational time is much lower.

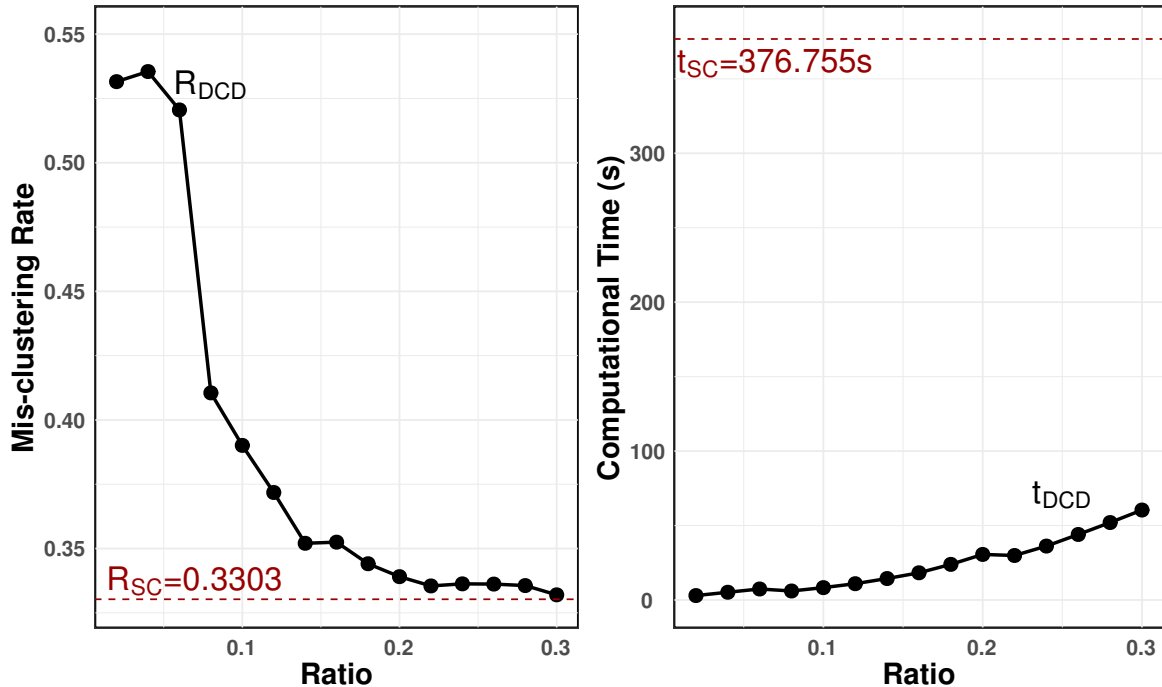


Figure 7: The Comparison between SC algorithm and DCD algorithm on Pubmed dataset both in mis-clustering rate and computational time. The mis-clustering rate and computational time of the DCD (SC) algorithm are denoted by R_{DCD} (R_{SC}) and t_{DCD} (t_{SC}) respectively.

5.2. Pokec Dataset: an Online Social Network

In this study, we consider a large scale social network, Pokec ([Takac and Zabovsky, 2012](#)). The Pokec is the most popular online social network in Slovak. The dataset was collected during May 25–27 in the year of 2012, which contains 50,000 active users in the network. If the i th user is a friend of the j th user, then there is a connection between the two users, i.e., $A_{ij} = 1$. The resulting network density is 0.0985%.

For the Pokec dataset, the network size is too huge for SC algorithm to output the result. As an alternative, we perform our DCD algorithm to conduct community detec-

tion. Since the memberships are not available, we produce another clustering criterion instead. Specifically, define the relative density as $RED = Den_{between}/Den_{within}$, where $Den_{between} = \sum_{i,j} a_{i,j} I(\hat{g}_i \neq \hat{g}_j) / \sum_{i,j} I(\hat{g}_i \neq \hat{g}_j)$ is the between-community density, and $Den_{within} = \sum_{i,j} a_{i,j} I(\hat{g}_i = \hat{g}_j) / \sum_{i,j} I(\hat{g}_i = \hat{g}_j)$ is the within-community density. The RED is visualized in Figure 8. As one can observe, after $l/N \geq 0.28$, the RED is stable with the corresponding computational time as 642.524s. This further illustrates the computational advantage of the proposed DCD algorithm.

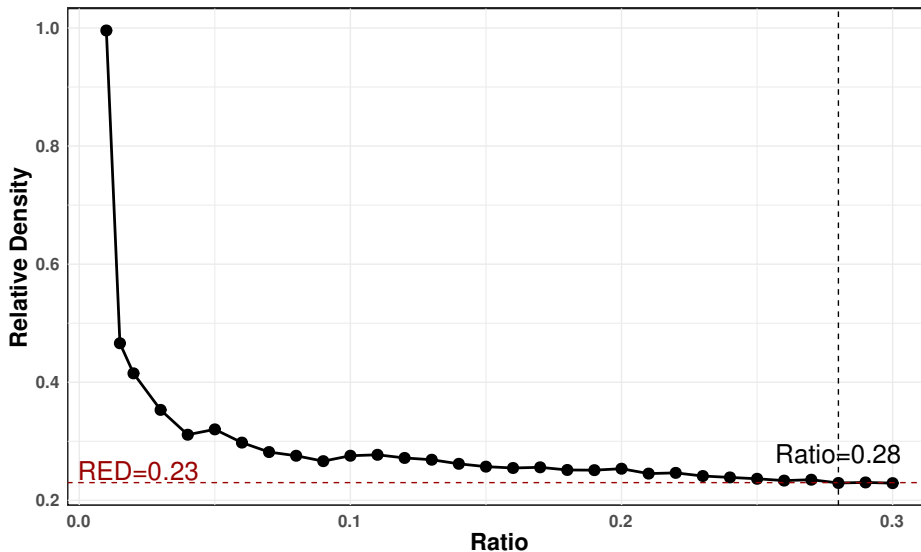


Figure 8: The relative density decreases rapidly as ratio increases, after $r = l/N \geq 0.28$, the RED is stable around 0.23.

6. CONCLUDING REMARKS

In this work, we propose a distributed community detection (DCD) algorithm to tackle community detection task in large scale networks. We distribute l pilot nodes on the master and a non-square adjacency matrix on workers. The proposed DCD algorithm has three merits. First, the communication cost is low. Second, no further iteration algorithm is used on workers therefore the algorithm is stable. Third, both

the computational complexity and the storage requirements are much lower compared to using the whole adjacency matrix. The DCD algorithm is shown to have clear computational advantage and competitive statistical performance by using a variety synthetic and empirical datasets.

To conclude the article, we provide several topics for future studies. First, better mechanisms can be designed to select pilot nodes on the master server. This enables us to obtain more accurate estimation of the pseudo centers and yields better clustering results. Next, it is interesting to extend the proposed method to directed network by considering sending and receiving clusters respectively (Rohe et al., 2012). The theoretical property and computational complexity could be discussed accordingly. Third, in the community detection task, we only employ the network structure information and ignore other potential useful nodal covariates. As a result, it is important to extend the DCD algorithm to further incorporate various exogenous information.

References

- Amini, A. A., Chen, A., Bickel, P. J., Levina, E., et al. (2013), “Pseudo-likelihood methods for community detection in large sparse networks,” *The Annals of Statistics*, 41, 2097–2122.
- Anandkumar, A., Ge, R., Hsu, D., and Kakade, S. M. (2014), “A tensor approach to learning mixed membership community models,” *The Journal of Machine Learning Research*, 15, 2239–2312.
- Balakrishnan, S., Xu, M., Krishnamurthy, A., and Singh, A. (2011), “Noise thresholds for spectral clustering,” in *Advances in Neural Information Processing Systems*, pp. 954–962.

- Battey, H., Fan, J., Liu, H., Lu, J., and Zhu, Z. (2015), “Distributed estimation and inference with statistical guarantees,” *arXiv preprint arXiv:1509.05457*.
- Bickel, P. J. and Chen, A. (2009), “A nonparametric view of network models and Newman–Girvan and other modularities,” *Proceedings of the National Academy of Sciences*, 106, 21068–21073.
- Chang, X., Lin, S.-B., and Wang, Y. (2017a), “Divide and conquer local average regression,” *Electronic Journal of Statistics*, 11, 1326–1350.
- Chang, X., Lin, S.-B., and Zhou, D.-X. (2017b), “Distributed semi-supervised learning with kernel ridge regression,” *The Journal of Machine Learning Research*, 18, 1493–1514.
- Chen, Y., Sanghavi, S., and Xu, H. (2012), “Clustering sparse graphs,” in *Advances in neural information processing systems*, pp. 2204–2212.
- Fan, J., Wang, D., Wang, K., and Zhu, Z. (2017), “Distributed estimation of principal eigenspaces,” *arXiv preprint arXiv:1702.06488*.
- Härdle, W. K., Wang, W., and Yu, L. (2016), “Tenet: Tail-event driven network risk,” *Journal of Econometrics*, 192, 499–513.
- Holland, P. W., Laskey, K. B., and Leinhardt, S. (1983), “Stochastic blockmodels: First steps,” *Social networks*, 5, 109–137.
- Jin, J. et al. (2015), “Fast community detection by SCORE,” *The Annals of Statistics*, 43, 57–89.
- Jordan, M. I., Lee, J. D., and Yang, Y. (2018), “Communication-efficient distributed statistical inference,” *Journal of the American Statistical Association*, 1–14.

- Kipf, T. N. and Welling, M. (2016), “Semi-supervised classification with graph convolutional networks,” *arXiv preprint arXiv:1609.02907*.
- Lee, J. D., Sun, Y., Liu, Q., and Taylor, J. E. (2015), “Communication-efficient sparse regression: a one-shot approach,” *arXiv preprint arXiv:1503.04337*.
- Lei, J. and Rinaldo, A. (2015), “Consistency of spectral clustering in stochastic block models,” *The Annals of Statistics*, 43, 215–237.
- Lei, L., Li, X., and Lou, X. (2020), “Consistency of Spectral Clustering on Hierarchical Stochastic Block Models,” *arXiv preprint arXiv:2004.14531*.
- Liu, Q. and Ihler, A. T. (2014), “Distributed estimation, information loss and exponential families,” in *Advances in neural information processing systems*, pp. 1098–1106.
- Liu, X., Patacchini, E., and Rainone, E. (2017), “Peer effects in bedtime decisions among adolescents: a social network model with sampled data,” *The econometrics journal*, 20, S103–S125.
- Marbach, D., Costello, J. C., Küffner, R., Vega, N. M., Prill, R. J., Camacho, D. M., Allison, K. R., Kellis, M., Collins, J. J., and Stolovitzky, G. (2012), “Wisdom of crowds for robust gene network inference,” *Nature methods*, 9, 796–804.
- Marbach, D., Prill, R. J., Schaffter, T., Mattiussi, C., Floreano, D., and Stolovitzky, G. (2010), “Revealing strengths and weaknesses of methods for gene network inference,” *Proceedings of the national academy of sciences*, 107, 6286–6291.
- Rohe, K., Chatterjee, S., Yu, B., et al. (2011), “Spectral clustering and the high-dimensional stochastic blockmodel,” *The Annals of Statistics*, 39, 1878–1915.
- Rohe, K., Qin, T., and Yu, B. (2012), “Co-clustering for directed graphs: the Stochastic co-Blockmodel and spectral algorithm Di-Sim,” *arXiv preprint arXiv:1204.2296*.

- Sarkar, P., Bickel, P. J., et al. (2015), “Role of normalization in spectral clustering for stochastic blockmodels,” *The Annals of Statistics*, 43, 962–990.
- Sojourner, A. (2013), “Identification of peer effects with missing peer data: Evidence from Project STAR,” *The Economic Journal*, 123, 574–605.
- Takac, L. and Zabovsky, M. (2012), “Data analysis in public social networks,” in *International scientific conference and international workshop present day trends of innovations*, vol. 1.
- Von Luxburg, U. (2007), “A tutorial on spectral clustering,” *Statistics and computing*, 17, 395–416.
- Zhang, Y., Duchi, J. C., and Wainwright, M. J. (2013), “Communication-efficient algorithms for statistical optimization,” *The Journal of Machine Learning Research*, 14, 3321–3363.
- Zhao, Y., Levina, E., Zhu, J., et al. (2012), “Consistency of community detection in networks under degree-corrected stochastic block models,” *The Annals of Statistics*, 40, 2266–2292.
- Zhu, X., Huang, D., Pan, R., and Wang, H. (2020), “Multivariate spatial autoregressive model for large scale social networks,” *Journal of Econometrics*, 215, 591–606.
- Zhu, X., Li, F., and Wang, H. (2019), “Least Squares Approximation for a Distributed System,” *arXiv preprint arXiv:1908.04904*.
- Zou, T., Lan, W., Wang, H., and Tsai, C.-L. (2017), “Covariance regression analysis,” *Journal of the American Statistical Association*, 112, 266–281.